Int. J. Morphol.,
43(4):1388-1401, 2025.

Morphoquantitative Comparison of the Temporomandibular Joint in Laboratory Species: Rabbit, Guinea Pig, Rat and Mouse

Comparación Morfocuantitativa de la Articulación Temporomandibular en Especies de Laboratorio: Conejo, Cuye, Rata y Ratón

Javiera Navarrete[1]; Francisco Mendoza[2]; Veronica Iturriaga[3,4,5]; Schilin Wen[6] & Bélgica Vásquez[5,7]

NAVARRETE, J.; MENDOZA, F.; ITURRIAGA, V.; WEN, S. & VÁSQUEZ, B. Morphoquantitative comparison of the temporomandibular joint in laboratory species: rabbit, guinea pig, rat and mouse. *Int. J. Morphol., 43(4)*:1388-1401, 2025.

SUMMARY: The temporomandibular joint (TMJ) is frequently affected by temporomandibular disorders (TMD). The selection of an animal model should be based on morphological features comparable to the human TMJ; however, few detailed comparative studies across commonly used laboratory species are available. This study aimed to compare the histological and morphometric characteristics of the TMJ in rabbit, guinea pig, rat, and mouse, to identify relevant structural differences that may guide the choice of animal models in TMD research. TMJs from four species (n = 4 joints per group) were maintained under controlled conditions. Following euthanasia, specimens were fixed, decalcified in 10 % EDTA, and processed for histology. Parasagittal sections (5 μm) were stained with toluidine blue and Picrosirius red. Histological analysis focused on the mandibular fossa (MF), articular disc (AD), and mandibular condyle (MC). A standardized morphometric protocol was applied to measure total thickness in the anterior (AR), middle (MR), and posterior (PR) regions, as well as in the tangential (TZ), transitional (TrZ), radial (RZ), and calcified cartilage (CC) zones of the condylar cartilage across the three anatomical regions. The species exhibited differences in cartilage zonation, cellular density, and structural organization. Rabbits and guinea pigs showed a well-defined zonal organization and greater cationic staining of the matrix, whereas rats and mice exhibited reduced zonal differentiation. With Picrosirius red, rabbits and guinea pigs displayed intense birefringence in the AD, while in mice it was weak and scattered. Morphometrically, rabbits generally exhibited the greatest thickness values and mice the lowest, although each species displayed a unique regional pattern. Rabbits consistently showed the highest values in the RZ and CC across all regions. The histoarchitectural and morphometric differences reflect specific biomechanical adaptations. Rabbits and guinea pigs appear to be more suitable for studies involving high mechanical load and complex fibrocartilage, rats may be useful for investigating mechanical adaptation and malocclusion due to their intermediate structure and condylar asymmetry, whereas mice are appropriate for genetic and molecular studies because of their structural homogeneity and the availability of transgenic models.

KEY WORDS: Temporomandibular joint; Histology; Morphometry; Animal models.

INTRODUCTION

The temporomandibular joint (TMJ) is a synovial joint with a highly specialized morphofunctional organization that enables complex movements such as mastication, swallowing, and speech (Matamala *et al*., 2006; Bechtold *et al*., 2016). This anatomical and functional complexity makes it particularly vulnerable to a wide spectrum of clinical alterations grouped under the term temporomandibular disorders (TMD), whose multifactorial etiology and variable clinical presentation complicate diagnosis and treatment (Ukita *et al*., 2020). In this context, animal models are essential tools for studying TMJ physiology and pathology, and their selection depends on multiple criteria, including morphofunctional similarity to humans, ease of handling, and the biological features inherent to each species (Herring *et al*., 2002; Cougo *et al*., 2021).

[1] Doctoral Program in Morphological Sciences, Faculty of Medicine, Universidad de La Frontera, Temuco, Chile.
[2] School of Medical Technology, Faculty of Medicine, Universidad de La Frontera, Temuco, Chile.
[3] Department of Integral Adult Care Dentistry, Temporomandibular Disorder and Orofacial Pain Program, Universidad de La Frontera, Temuco, Chile.
[4] Sleep & Pain Research Group, Universidad de La Frontera, Temuco, Chile.
[5] Center of Excellence in Morphological and Surgical Studies, Universidad de La Frontera, Temuco, Chile.
[6] Undergraduate Research Group in Dentistry, Faculty of Health Sciences (FACSA), Universidad Autónoma de Chile, Temuco, Chile.
[7] Department of Basic Sciences, Faculty of Medicine, Universidad de La Frontera, Temuco, Chile.
FUNDED. Partially funded by the Research Directorate, Universidad de La Frontera, Support PP24-0034.

Received: 2025-05-14 Accepted: 2025-07-02

From an anatomical perspective, the human TMJ is formed superiorly by the mandibular fossa (MF), an oval depression in the squamous portion of the temporal bone, together with the articular tubercle (AT), which delimit the osseous roof of the joint. Inferiorly, it articulates with the mandibular condyle (MC), an ellipsoid prominence located at the superior end of the mandibular ramus (Okeson, 2013; Palla, 2016).

Between these two osseous structures lies the articular disc (AD), a key fibrocartilaginous structure that divides the joint cavity into two functional compartments: a superior compartment that allows translational movements and an inferior compartment related to rotational movements. The shape of the AD adapts to the articular surfaces; in general, its superior surface, in contact with the MF and AT of the temporal bone, is concavo-convex, whereas its inferior surface, in relation to the MC, is concave (Wurgaft & Montenegro, 2003).

The TMJ is surrounded by a fibrous articular capsule, which attaches to the margins of the MF and MC, providing structural containment. Inside the capsule lies the synovial membrane, a thin and vascularized lining located at the lateral aspects of the superior and inferior compartments of the articular cavity. Its main function is to produce synovial fluid (SF), which lubricates and nourishes the avascular articular surfaces. The joint complex is stabilized by intrinsic and extrinsic ligaments (Tomas *et al*., 2007; Porto *et al*., 2010; Palla, 2016). In addition, the dynamic function of the TMJ is closely related to the coordinated action of the masticatory muscles—particularly the masseter, temporalis, and the lateral and medial pterygoid muscles—which enable mandibular movements such as opening, closing, protrusion, retrusion, and laterality. The integration of all these components allows the TMJ to perform both rotational and translational movements in a coordinated manner, which are essential for its proper function (Matamala *et al*., 2006; Tomas *et al*., 2007; Okeson, 2013; Palla, 2016; Tomasello *et al*., 2016; Cougo *et al*., 2021).

Histologically, in adult humans, the articular surface of the MF is covered by dense fibrous connective tissue, lacking hyaline cartilage and a well-defined zonal organization, unlike other articular surfaces. However, during development, this region may transiently present a layered histological organization, with a tangential zone (TZ), followed by a transitional zone (TrZ), a radial zone (RZ), and, in some instances, calcified cartilage (CC). This arrangement reflects a phase of functional adaptation and tissue remodeling associated with growth (Wurgaft & Montenegro, 2003). The human AD is composed of fibrous connective tissue, which allows it to withstand multidirectional forces. In sagittal sections, four regions can be distinguished: anterior, intermediate, posterior, and retrodiscal. The intermediate zone, the thinnest, is formed by dense fibrous connective tissue and lacks vascularization and innervation, suggesting a functional adaptation to withstand maximal compressive loads (Okeson, 2013; Palla, 2016; Dellavia *et al*., 2019). In young individuals, isolated chondrocytes may be observed in the intermediate zone, suggesting a degree of adaptive cartilaginization of the tissue (Wurgaft & Montenegro, 2003). The osseous tissue of the MC is covered by articular cartilage, which cushions and distributes forces across the articular surface. This articular cartilage displays a stratified histological organization comprising four main zones: TZ, composed of dense connective tissue with type I collagen fibers oriented parallel to the articular surface; TrZ, containing undifferentiated mesenchymal cells with progenitor potential; RZ, characterized by columns of chondrocytes oriented perpendicularly to the articular surface, along with thick bundles of type I collagen extending into the underlying bone; and CC, which contains mature and hypertrophic chondrocytes involved in endochondral ossification (Okeson, 2013; Palla, 2016).

Animal models are indispensable for TMJ research, given the inherent limitations of obtaining human samples at different pathological stages and the need to control experimental variables (Porto *et al*., 2010; Cougo *et al*., 2021). These experimental models enable the study of pathogenesis, the development of diagnostic criteria, and the evaluation of therapeutic approaches, although none can fully replicate the morphofunctional characteristics of the human TMJ (Cougo *et al*., 2021; Zhao *et al*., 2022). This fundamental limitation underscores the importance of carefully selecting the most appropriate animal model for each specific research question (Zhao *et al*., 2022).

Rabbits (*Oryctolagus cuniculus*), guinea pigs (*Cavia porcellus*), rats (*Rattus norvegicus*), and mice (*Mus musculus*) are species frequently used in preclinical studies (Porto *et al*., 2010; Jung *et al*., 2014), particularly in research on mechanical injury or induced osteoarthritis (Iturriaga *et al*., 2021; Wen *et al*., 2023). However, these models present significant limitations (Jung *et al*., 2014; Zhao *et al*., 2022). Studies in rabbits do not always reproduce the expected severity of degenerative changes, and the induction of abrupt mechanical alterations may not adequately represent controlled occlusal modifications in humans. Conversely, chemically induced degenerative changes in rodents may fail to faithfully reproduce human pathological conditions (Cougo *et al*., 2021).

Given the remarkable interspecies variability and the absence of specific guidelines for selecting the optimal animal model (Porto *et al*., 2010; Zhao *et al*., 2022), a comparative study detailing the morphometric and histological characteristics of the TMJ across these organisms is justified (Berkovitz, 2000). Such systematic comparison will provide fundamental information to appropriately guide the choice of the most suitable animal model in future TMJ research and its associated pathologies (Herring, 2003; Cougo *et al*., 2021; Zhao *et al*., 2022).

Therefore, the present study aimed to perform a comparative histological and morphometric analysis of the TMJ in four laboratory species (rabbit, guinea pig, rat, and mouse) to identify the distinctive morphological features of each animal model and to establish objective criteria for selecting the most appropriate model according to the specific research objectives in the field of TMD.

MATERIAL AND METHOD

Animals.

Adult, healthy specimens of four laboratory species were used: rabbits (*Oryctolagus cuniculus*), guinea pigs (*Cavia porcellus*), rats (*Rattus norvegicus*), and mice (*Mus musculus*) (n = 4 TMJs per group). Animals were maintained under controlled environmental conditions of temperature, ambient noise, and a 12-hour light/12-hour dark cycle. They were housed individually in randomly assigned cages. The study was conducted at the Experimental Surgery Unit of the Center of Excellence in Morphological and Surgical Studies, Universidad de La Frontera, following the ARRIVE guidelines and the National Research Council's Guide for the Care and Use of Laboratory Animals (2011). The principles of replacement, reduction, and refinement (3Rs) established by Russell & Burch (1959) were observed to minimize the number of animals used. Following euthanasia, the TMJ tissues of all four species were dissected.

Histological processing.

Tissues were fixed in 10 % neutral buffered formalin (formaldehyde 1.27 mol/L in 0.1 M phosphate buffer, pH 7.2) for 48 hours. Samples were then decalcified in 10 % ethylenediaminetetraacetic acid (EDTA) (0.1 M phosphate buffer, pH 7–8) for 30 days. Decalcification was performed using an ultrasonic decalcifier (Use 33, Medite) to optimize the procedure. Decalcified tissues were dehydrated through ascending alcohols, cleared in xylene, and embedded in Paraplast Plus (Sigma-Aldrich Co.). Serial parasagittal sections of the TMJ were cut at 5 μm thickness using a rotary microtome (Leica® RM 2255).

For optimal evaluation, successive sections from the deepest planes of the joint were selected. Histological sections were mounted on slides and stained using two specific protocols: toluidine blue for general visualization of cartilaginous structures and extracellular matrix, and Picrosirius red for the specific identification of type I and type III collagen fibers. Sections were examined under a light microscope (Leica® DM750) and photographed with a digital camera (Leica® ICC50 HD).

Histological analysis

Histological assessment of the TMJs included the MF, AD, and MC. The articular cartilage was described from superficial to deep, using the following terminology: tangential zone (TZ), transitional zone (TrZ), radial zone (RZ), and calcified cartilage (CC). These histological zones of the condylar cartilage were identified and delimited according to standardized morphological and staining criteria with toluidine blue. The TZ was defined from the articular surface to the first appearance of rounded or isogenous chondrocytes. The TrZ extended from the end of the TZ to the beginning of columnar organization of hypertrophic chondrocytes. The RZ was defined from the end of the TrZ to the shift from purple metachromasia to the blue staining characteristic of CC. The CC was identified by the color change from purple to blue with toluidine blue and extended to the interface with the subchondral bone.

Morphometric analysis

The total thickness of the articular cartilage of the MC was measured in three anatomical regions: anterior region (AR), middle region (MR), and posterior region (PR). These regions corresponded to the initial, central, and final thirds of the MC in the anteroposterior direction. Delimitation was based on consistent anatomical landmarks across species, considering condylar curvature and its relationship to the subchondral bone. In each region of the MC, three measurements were taken at equidistant points. Additionally, the thickness of the different histological zones of the condylar cartilage, including the CC, was measured specifically in each region.

All measurements were performed under the same magnification (40×) and standardized illumination. Morphometric analyses of each sample were independently conducted by authors J. N. and F. M. Discrepancies were resolved through discussion and consensus. Each measurement was recorded in a specifically designed database, including animal identification code, condylar side, anatomical region, histological zone, and recorded values.

Statistical analysis

The data obtained from the total thickness and the different histological zones of the condylar cartilage were analyzed using SPSS software (version 27). The normality of the distribution was assessed with the Shapiro–Wilk test. Since most variables did not meet the assumption of normality, nonparametric tests were applied. Comparisons among the three regions of the condylar cartilage (anterior, middle, and posterior) within each species were performed using the Kruskal–Wallis test, followed by Dunn's correction for multiple comparisons. Inter-species comparisons were also conducted with Kruskal–Wallis, considering each region separately and applying the same post hoc procedure. Results were expressed as median ± interquartile range (IQR), and a p-value < 0.05 was considered statistically significant.

RESULTS

Histological analysis of the temporomandibular joint

The TMJs of the studied species exhibited diverse histological architecture, with notable differences in the degree of zonation, extracellular matrix organization, and cellular arrangement. These characteristics reflected varying degrees of tissue specialization and biomechanical adaptation (Fig. 1A-D).

Mandibular Fossa

In rabbits, the MF was the deepest among all species, with a clearly defined morphology. The articular surface was covered by dense connective tissue with type I collagen fibers oriented parallel to the articular plane. Moderate chondrogenic zonation was observed, with rounded chondrocytes in the TrZ and weak metachromasia in the RZ. A continuous CC was not observed, showing instead a direct transition into the temporal bone (Fig. 1E). Under Picrosirius red, the articular surface stained intensely red-orange, reflecting a dense and well-organized collagen network (Fig. 2A).

In guinea pigs, the MF was flatter than in rabbits, although well defined. The articular surface displayed dense connective tissue with well-organized type I collagen fibers and strong birefringence. Histologically, chondrocytes were present in the TrZ, and the RZ showed a clear transition into the CC (Fig. 1F). Collagen type I in the surface exhibited strong red-orange birefringence, although less compact than in rabbits (Fig. 2B).

In rats, the MF architecture was less compact, with weak zonal differentiation. The TZ consisted of dense connective tissue with type I collagen fibers. Slight metachromasia was noted in the TrZ, increasing slightly in the RZ. The CC was irregular, showing a wavy transition into the temporal bone (Fig. 1G). With Picrosirius red, birefringence was weak and in green-yellowish tones, suggesting lower collagen density and organization (Fig. 2C).

In mice, the MF was the thinnest and least differentiated. It exhibited dense connective tissue with type I collagen fibers lacking clear orientation. Zonation was difficult to distinguish, and the transition into the bone was abrupt yet regular (Fig. 1H). Picrosirius red revealed very faint birefringence in green tones, indicative of type III collagen and/or poorly organized type I collagen (Fig. 2D).

Overall, a gradient of structural complexity was evident from rabbit to mouse. Rabbits and guinea pigs showed a more robust and organized articular surface, whereas rats and mice exhibited simpler architecture with lower collagen density and organization (Table I).

Articular Disc

In rabbits, the AD was composed of avascular fibrocartilage, consisting mainly of thick, dense bundles of type I collagen arranged parallel to each other, with chondrocytes aligned according to fiber orientation. Its well-defined biconcave morphology displayed marked concavities on both surfaces, with progressive thickening toward the capsular insertions. Sagittal sections stained with toluidine blue revealed the most complex organization in the central region, with intense and homogeneous metachromasia. Central chondrocytes had round to oval nuclei, aligned axially, each surrounded by a well-defined pericellular metachromatic matrix, without evidence of isogenous groups. Toward the periphery, an abrupt transition was observed: metachromasia markedly decreased, and the fibrillar network became loose and irregular, with variable orientation compatible with a circumferential pattern. Peripheral cells were scarce and consisted exclusively of fusiform fibroblasts with elongated nuclei aligned with the fibers (Fig. 1I). With Picrosirius red, the periphery showed strong red-orange birefringence, while the central region exhibited continuous, intense red birefringence, reflecting a densely organized type I collagen matrix oriented mainly in the anteroposterior direction (Fig. 2A).

In guinea pigs, the AD had a well-defined biconcave morphology, with intermediate thickness compared to the other species analyzed. Structurally, it was distinct, characterized by a heterogeneous and less compact fibrillar matrix than in rabbits. In the central zone, thin bundles of type I collagen with irregular trajectories (curved, divergent, and interwoven) were observed, generating a disorganized

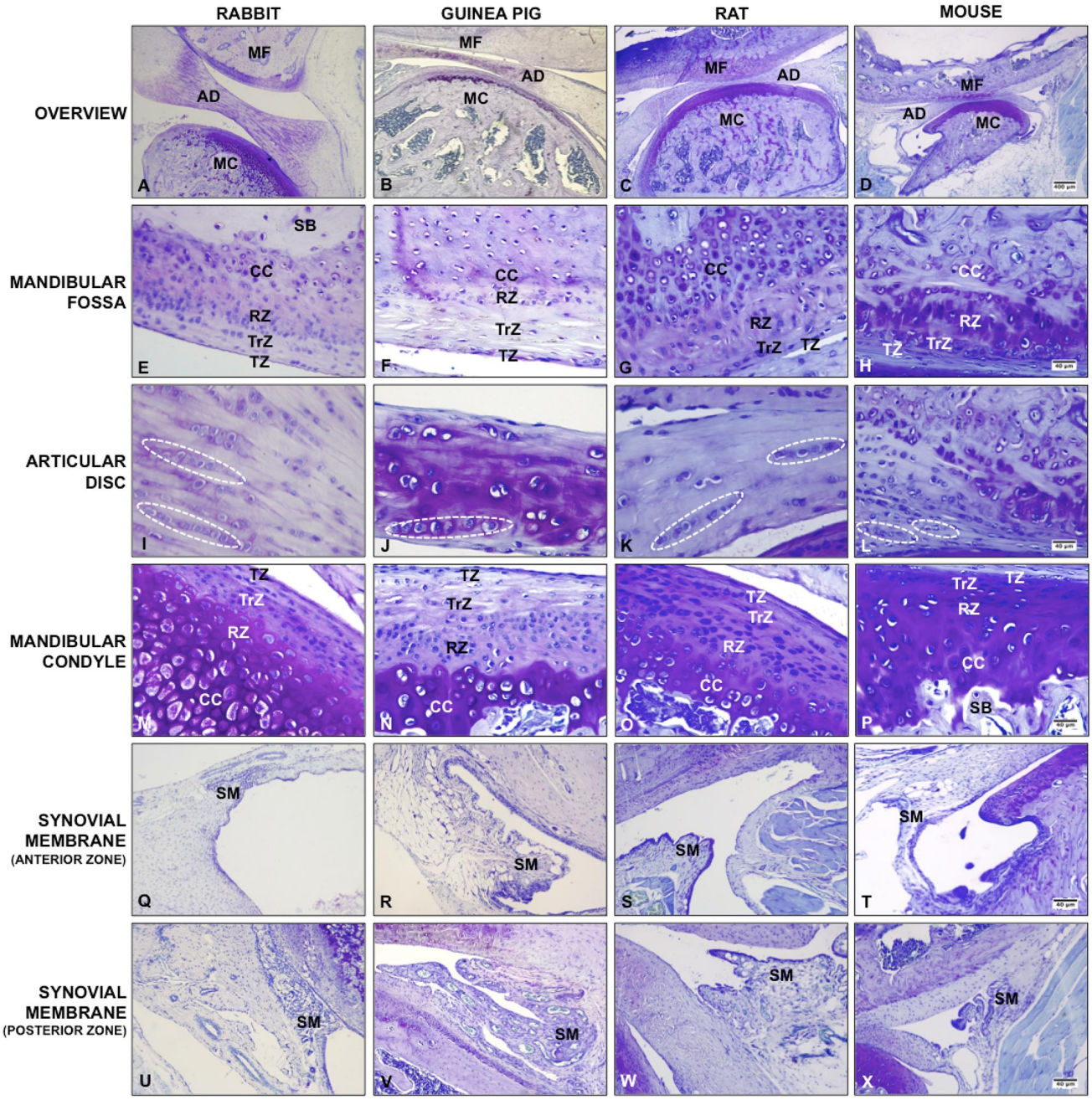

Fig. 1. Temporomandibular joint of rabbit (*Oryctolagus cuniculus*), guinea pig (*Cavia porcellus*), rat (*Rattus norvegicus*), and mouse (*Mus musculus*). Mandibular fossa (MF), articular disc (AD), mandibular condyle (MC), synovial membrane (SM), tangential zone (TZ), transitional zone (TrZ), radial zone (RZ), calcified cartilage (CC), subchondral bone (SB), dotted line area (chondrocytes arranged in axial isogenous groups). Toluidine blue staining.

but still functionally coherent pattern. Metachromasia in this region was moderate, greater than that observed in rats and mice but lower than in rabbits. Central chondrocytes appeared dispersed, with round to oval nuclei, surrounded by variably metachromatic pericellular matrix. Numerous fusiform fibroblasts were present among the collagen bundles. Toward the periphery, the fibrillar network became looser, lacking sagittal orientation, and was composed exclusively of scarce fibroblasts (Fig. 1J). With Picrosirius red, the central region showed fibrillar trajectories oriented anteroposteriorly, with intermediate birefringence ranging from green-yellow to pale orange, suggesting a looser but structured matrix. In contrast, the periphery exhibited stronger red-orange birefringence, indicative of densely packed type I collagen (Fig. 2B).

Table I. Comparison of the histological characteristics of the temporomandibular joint in rabbit (*Oryctolagus cuniculus*), guinea pig (*Cavia porcellus*), rat (*Rattus norvegicus*), and mouse (*Mus musculus*).

Estructure		Rabbit	Guinea pig	Rat	Mouse
Mandibular fossa.	TZ	Dense connective tissue with well-organized, parallel type I collagen fibers; flattened fibroblasts; scarce metachromasia.	Similar to rabbit, but with lower fiber density; thinner fibers and scattered fibroblasts.	Connective tissue with less organized, irregularly arranged fibers; few fibroblasts; faint metachromasia.	Very thin; collagen fibers without clear orientation; occasional fibroblasts.
	TrZ	Rounded chondrocytes with slight metachromasia.	Transitioning chondrocytes; relatively organized collagen fibers.	Scattered chondrocytes; reduced fibrillar organization; mild metachromasia.	Poorly distinguishable zone; few chondrocytes; faint metachromasia.
	RZ	Low metachromasia and direct transition into temporal bone.	Defined transition into calcified cartilage; maturing chondrocytes.	Faint metachromasia and irregular transition into temporal bone.	Abrupt but regular transition into temporal bone.
	CC	Poorly defined and discontinuous calcified cartilage zone.	Present, continuous, and symmetrical.	Irregular and poorly defined.	Absent or barely visible.
Articular disc	CZ	Dense fibrocartilage; thick collagen bundles arranged anteroposteriorly; abundant chondrocytes; intense metachromasia; greatest thickness.	Less compact collagen, thinner bundles with irregular sagittal orientation; scattered chondrocytes; moderate metachromasia; intermediate thickness.	Thinner fibrocartilage; fine collagen bundles, parallel in anteroposterior orientation but less compact; aligned chondrocytes; moderate metachromasia.	Very thin; fine and loosely packed collagen bundles in anteroposterior orientation; few chondrocytes; mild to moderate metachromasia.
	PZ	Loose collagen fibers with irregular orientation (circumferential pattern); few fusiform fibroblasts; mild metachromasia.	Lower fiber density; loosely packed fibers with no defined orientation; few fibroblasts; mild metachromasia.	Loose fibers with no defined orientation; few fibroblasts; faint metachromasia.	Sparse, disorganized fibers; very low cellularity; occasional fibroblasts; minimal metachromasia.
Mandibular condyle	TZ	2 - 3 layers of highly flattened fibroblasts with densely organized parallel collagen fibers; no metachromasia.	2 - 3 layers of fibroblasts with slightly wavy parallel fibers; mild metachromasia.	1 - 2 layers of fibroblasts with loose, parallel fibers; mild metachromasia.	Single layer of flattened nuclei; dense fibers; no metachromasia.
	TrZ	Isolated chondrocytes and isogenous groups; intense metachromasia.	High cell density; defined isogenous groups; mild metachromasia.	Small isogenous groups; mild metachromasia.	Defined isogenous groups; intense metachromasia.
	RZ	Hypertrophic chondrocytes in incomplete columns; heterogeneous metachromasia.	Hypertrophic chondrocytes aligned in regular columns; intense, uniform metachromasia.	Isolated chondrocytes without columnar organization; mild metachromasia.	Short columns of hypertrophic chondrocytes; moderate metachromasia.
	CC	Irregular; necrotic hypertrophic chondrocytes surrounded by calcified matrix; no tidemark.	Well-developed and continuous; calcified cartilage present, continuous, and delimited by tidemark.	Diffuse; poorly defined transition; no tidemark.	Thin and uniform; difficult to identify; diffuse transition.

TZ: tangential zone; TrZ: transitional zone; RZ: radial zone; CC: calcified cartilage; CZ: central zone; PZ: peripheral zone.

In rats, the AD appeared as a thin but well-defined fibrocartilaginous structure, with a less pronounced biconcave morphology compared to rabbits and guinea pigs. In the central region, its organization was intermediate between the compactness of rabbits and the heterogeneity of guinea pigs. Metachromasia was moderate, and type I collagen

bundles were predominantly aligned anteroposteriorly, though less compact than in rabbits. Chondrocytes were the main cellular component, distributed individually among the fibers, with round to oval nuclei and pericellular matrix showing weak focal metachromasia, indicating moderate proteoglycan content. Dispersed fibroblasts with elongated nuclei aligned with the collagen bundles were also observed. The peripheral zone exhibited a looser fibrillar network, lacking sagittal orientation, suggesting a less structured circumferential pattern (Fig. 1K). With Picrosirius red, the central region exhibited predominantly green birefringence, consistent with type III collagen or poorly organized type I collagen. In contrast, peripheral fibers showed focal reddish birefringence, less continuous than in guinea pigs, suggesting lower fibrillar density and organization (Fig. 2C).

In mice, the AD was the thinnest and simplest structure among the species analyzed, with barely perceptible biconcavity and an almost flat contour. In the central zone, metachromasia was weak to moderate, the lowest observed, indicating poor proteoglycan content. Type I collagen fibers were arranged in very thin, loosely packed bundles with only minimal anteroposterior orientation. Chondrocytes were scarce, with small rounded nuclei and minimal pericellular metachromasia, without evidence of clustering or isogenous groups. No clear fibrillar transitions or internal zonation were observed. At the periphery, metachromasia was even weaker, with a network of thin fibers lacking defined orientation. Peripheral cells consisted exclusively of fusiform fibroblasts in very low density. Overall, zonal organization was poorly evident, showing the least fibrillar compactness and cellularity among all species studied (Fig. 1L). With Picrosirius red, both central and peripheral regions exhibited weak and inconsistent birefringence, predominantly in green tones, indicating a poorly dense and disorganized collagen matrix (Fig. 2D).

From a general perspective, rabbits and guinea pigs exhibited ADs with greater structural complexity and fibrillar organization. Rabbits stood out for their robustness and homogeneous intense metachromasia, while guinea pigs displayed a heterogeneous fibrillar pattern. In contrast, rats and mice presented thinner and simpler discs, with less collagen organization and weaker birefringence (Table I).

Mandibular Condyle

In rabbits, the MC exhibited an elongated oval morphology, with a smooth, continuous articular surface and well-defined histological zonation. The TZ was composed of multiple layers of flattened fibroblasts arranged parallel to the articular surface, accompanied by collagen fibers oriented in the same direction. In the TrZ, rounded chondrocytes were observed, distributed individually or in small isogenous groups with irregular arrangement. This zone showed progressive metachromasia, ranging from light violet to deep purple, reflecting a gradual increase in proteoglycans. The RZ exhibited hypertrophic chondrocytes organized in incomplete cellular columns, connected to a thick CC. No distinct tidemark was present, indicating a gradual transition into subchondral bone (Fig. 1M). Picrosirius red revealed zonal collagen organization: the TZ showed strong red-orange birefringence; the TrZ displayed yellow-orange hues; the RZ showed diffuse green-yellow birefringence; and the CC lacked birefringence, indicating absence of organized collagen fibers in this zone (Fig. 2A).

In guinea pigs, the MC morphology was similar to that of rabbits but with thinner articular cartilage. Clear histological zonation was observed. The TZ contained two to three layers of flattened fibroblasts with wavy collagen fibers oriented parallel to the articular surface. The TrZ exhibited the highest cellular density among the species, with well-defined isogenous groups (two to four cells) and intense purple metachromasia. The RZ showed perfectly aligned hypertrophic chondrocytes, with gradual transition into a continuous, symmetrical, and well-delimited CC (Fig. 1N). With Picrosirius red, three fibrillar zones were clearly distinguished: TZ (intense red birefringence), TrZ (yellow-orange), and RZ (diffuse green-yellow) (Fig. 2B).

In rats, the MC was round in shape, and although histological zones could be identified, their boundaries were less clear compared to rabbits and guinea pigs. The TZ consisted of one or two layers of flattened fibroblasts accompanied by loose, parallel collagen fibrils. No remarkable regional variations were noted, and cellular density was low and uniform. In the TrZ, a slight increase in cellular density was observed, with small isogenous groups (two to three cells) of diffuse boundaries. Metachromasia was homogeneous but weak (light violet), with poorly defined pericellular halos. Chondrocytes lacked evident columnar arrangement. The RZ displayed isolated hypertrophic chondrocytes, without alignment or columnar pattern. The transition into CC was diffuse and poorly defined, representing less than 5% of total cartilage thickness, without a clear tidemark (Fig. 1O). With Picrosirius red, the TZ exhibited weak green-yellow birefringence corresponding to thin collagen fibrils oriented partially parallel to the surface. The TrZ and RZ displayed very faint or absent birefringence, suggesting poorly organized collagen matrix. The CC lacked birefringence entirely (Fig. 2C).

In mice, the MC was the simplest and most homogeneous structure among the species studied, with the thinnest articular cartilage. Morphologically, it was small and rounded, with a smooth, regular articular surface. Cartilage

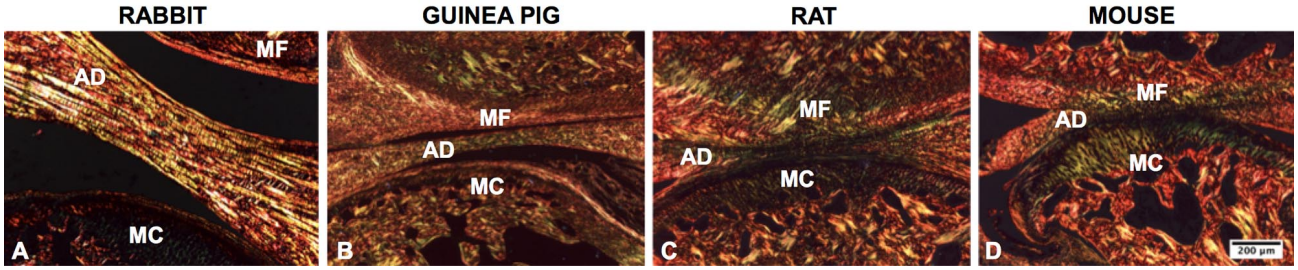

Fig. 2. Temporomandibular joint of rabbit (*Oryctolagus cuniculus*), guinea pig (*Cavia porcellus*), rat (*Rattus norvegicus*), and mouse (*Mus musculus*). Mandibular fossa (MF), articular disc (AD), mandibular condyle (MC). Picrosirius Red staining.

matrix stained uniformly with toluidine blue, making histological zonation difficult to distinguish, although relatively high proteoglycan content was evident. The TZ was absent or extremely reduced in most samples. When identifiable, it consisted of a single layer of flattened nuclei accompanied by densely packed collagen fibrils aligned with the surface. The TrZ showed better definition, with small isogenous groups of two to three well-delimited chondrocytes, distributed individually or clustered, with uniform pericellular halos and intense homogeneous purple metachromasia. The matrix was moderately organized without remarkable regional variations. The RZ, though thin, exhibited short columns of hypertrophic chondrocytes, aligned without clear transitional zones. Metachromasia remained intense and homogeneous, suggesting relatively high proteoglycan concentration despite reduced cartilage volume. The CC was inconsistently identifiable across samples and showed diffuse boundaries (Fig. 1P). With Picrosirius red, the articular surface revealed a dense collagen layer with fibers organized parallel to the surface. Strong continuous red-orange birefringence was observed, consistent with densely packed type I collagen. Toward deeper zones, birefringence intensity decreased gradually, without clearly defined fibrillar transitions, reflecting a less structured matrix compared to morphologically more complex species (Fig. 2D).

The comparative analysis revealed a gradient of structural complexity from rabbit to mouse. Rabbits and guinea pigs exhibited condyles with well-defined zonation, greater cellular density, and organized extracellular matrix, whereas rats and mice presented simpler architecture with less zonal differentiation and less organized cellular distribution. Each model displayed distinctive histological traits: greater thickness and fibrillar complexity in rabbits, exceptional cellular density and columnar organization in guinea pigs, condylar asymmetry in rats, and relative structural simplicity in mice, characterized by thin cartilage and poor zonation (Table I).

Interspecies comparison of condylar thickness by anatomical region and zonal thickness of condylar cartilage

In the AR of the MC, thickness was similar among rabbits, guinea pigs, and rats, with comparable values. Mice exhibited the lowest thickness in this region, with significant differences compared to guinea pigs. In the MR, rabbits recorded the greatest condylar thickness, followed by guinea pigs. Rats and mice showed lower and comparable values. Statistically significant differences were observed with rabbits. In the PR, the greatest thickness was found in rabbits, with significant differences compared to guinea pigs and mice. Taken together, these findings indicate that although there is a general trend toward greater condylar thickness in rabbits and lower values in mice, each species displayed a unique regional distribution profile of the articular cartilage. These differences are represented in Figure 3, which shows the median values of articular cartilage thickness in the three anatomical regions of the MC for each species.

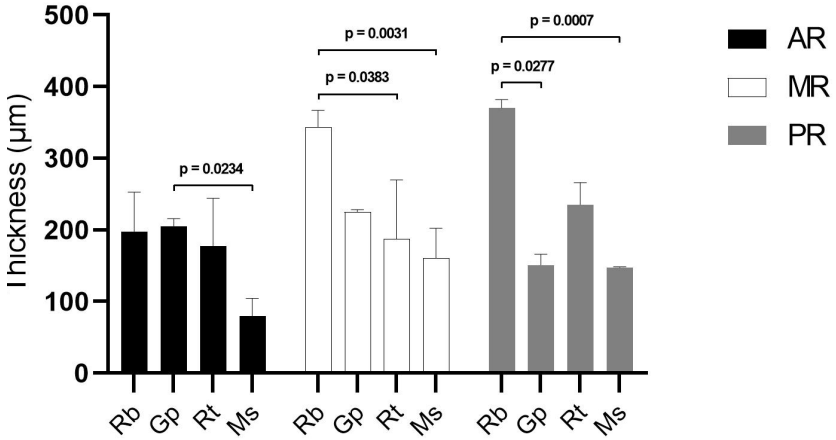

Fig. 3. Articular cartilage thickness of the mandibular condyle in the anterior (AR), middle (MR), and posterior (PR) regions in four laboratory species: rabbit (Rb), guinea pig (Gp), rat (Rt), and mouse (Ms). Results are expressed as median ± IQR, with $p < 0.05$ considered statistically significant.

With respect to zonal thickness, rabbits consistently exhibited the greatest thickness in the RZ and CC of the condylar cartilage across all anatomical regions. They also showed the greatest thickness in the TrZ within the PR. In contrast, mice exhibited the lowest values in almost all zones and regions analyzed, highlighting significant morphometric differences between the two extremes of the interspecies comparative model (Fig. 4).

DISCUSSION

This study provides a comparative histological and morphometric characterization of the MF, AD, and MC in four laboratory species widely used in biomedical research: rabbit (*Oryctolagus cuniculus*), guinea pig (*Cavia porcellus*), rat (*Rattus norvegicus*), and mouse (*Mus musculus*). Using conventional stains and differential collagen detection, we identified species-specific structural variations that correlate with functional differences and biomechanical adaptations. These findings are framed within the recognition of the TMJ as a highly specialized unit whose organization reflects the mechanical demands imposed by feeding habits and masticatory patterns (Shibata, 2014; Stocum & Roberts, 2018; Nanci, 2018).

In accordance with the objectives of the study, the discussion is organized by structure and then integrated into a functional, methodological, and model selection framework.

Mandibular Fossa

The MF displayed a spectrum of variations reflecting biomechanical adaptations and differences in the degree of specialization of the articular surface. Rabbits presented the deepest and most clearly delimited MF, covered by dense connective tissue rich in type I collagen fibers oriented parallel to the articular plane. This pattern is associated with surfaces exposed to high cyclic loading, in which fiber parallelism optimizes resistance to shear (Roberts & Goodacre, 2020). Moderate

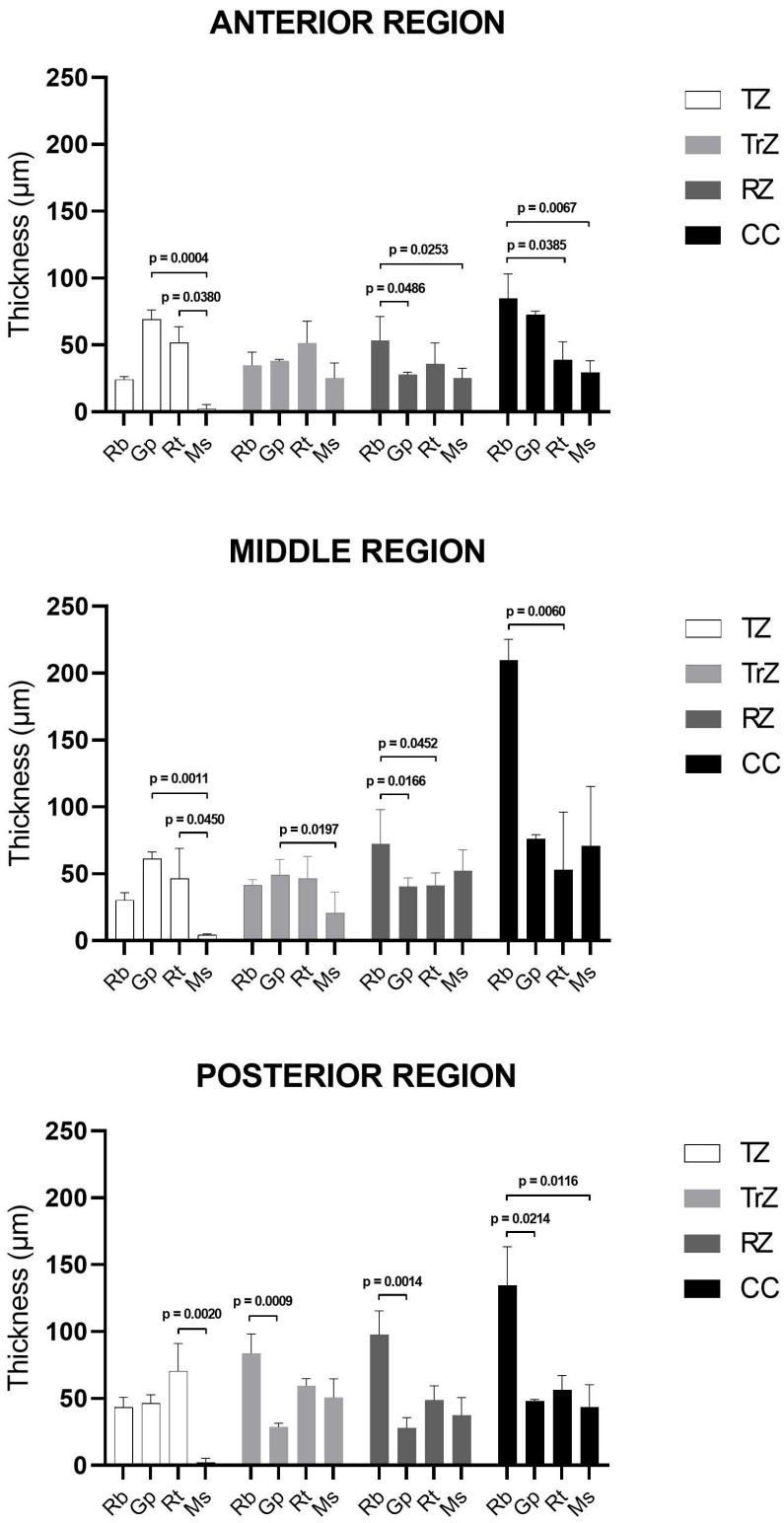

Fig. 4. Zonal thickness of the mandibular condylar cartilage in the anterior, middle, and posterior regions in rabbit (Rb), guinea pig (Gp), rat (Rt), and mouse (Ms). Individual thickness values are shown for the tangential zone (TZ), transitional zone (TrZ), radial zone (RZ), and calcified cartilage (CC), expressed in micrometers. Results are expressed as median ± IQR, with $p < 0.05$ considered statistically significant.

chondrogenic zonation, rounded chondrocytes in the TrZ and weak metachromasia in the RZ, suggests a balance between mechanical resistance and limited damping capacity. The absence of a continuous CC, with a direct transition into temporal bone, may facilitate rapid remodeling in response to load changes, as occurs in animals with variable masticatory patterns (Stocum & Roberts, 2018).

In contrast, guinea pigs showed a shallower MF but with a well-organized fibrous lining and greater TrZ metachromasia, suggesting a higher proteoglycan contribution and, therefore, greater cushioning than in rabbits. Rats had a shallower MF with a less compact surface tissue characterized by looser fibers and lower type I collagen density, consistent with lower masticatory demand given dietary pattern and mandibular size. Mice exhibited the simplest and least defined MF, with thin collagen fibers and a generally less specialized organization, reflecting lower functional demand and a simplified TMJ in small species (Porto *et al*., 2010; Suzuki & Iwata, 2016).

Functionally, interspecies differences in the MF may substantially influence the mechanics of the superior compartment, where translation and sliding depend on the integrity and organization of the fibrous covering. Rabbits and guinea pigs are thus more robust models for studies assessing changes in functional load and their impact on the MF, whereas rats and mice offer simplified models suitable for basic investigations of articular tissue biology.

Articular Disc

The AD exhibited structural variability closely correlated with functional demands and biomechanical complexity. In rabbits, the AD showed a dense collagen architecture with fibers predominantly oriented anteroposteriorly and strong birefringence under polarized light, compatible with well-packed type I collagen. This architecture suggests high resistance to compression and shear, consistent with complex masticatory movements (Chen *et al*., 2020; Roberts & Goodacre, 2020). The homogeneous staining and limited regional variability indicate mechanically uniform properties that evenly distribute loads throughout its thickness.

Guinea pigs presented intermediate collagen compactness but higher cellular density and more evident metachromasia than rabbits, suggesting higher proteoglycan content and thus greater damping capacity. Fiber arrangement showed more marked regional organization, denser in the intermediate zone and looser at the periphery, potentially reflecting adaptation to directional loads.

In rats, the AD showed lower collagen density and less organized fibers with more heterogeneous staining, indicative of a matrix with lower mechanical resistance and greater susceptibility to deformation under prolonged load. In mice, the AD was the thinnest and simplest, with thin fibers, low cellular density, and moderate birefringence, reflecting a more basic mechanical role with less structural specialization. Because disc composition and architecture determine energy absorption and resistance to plastic deformation (Chen *et al*., 2020), the high homogeneity observed in mice may explain their lower tolerance to repetitive loading and susceptibility to deformation under experimental overload.

Mandibular Condyle

The MC is the most morphologically and functionally variable TMJ component, and our results confirm a hierarchical gradient in thickness and histological complexity following rabbit > guinea pig > rat > mouse. Rabbits exhibited clearly defined zones: a fibrous TZ, a TrZ rich in isogenous chondrocyte groups, an RZ with organized hypertrophic chondrocytes, and a well-delimited, relatively thick CC. This architecture supports high capacity for load absorption and redistribution and agrees with reports of a highly adaptive condylar pattern in rabbits (Shibata *et al*., 2014). Intense metachromasia in the TrZ and RZ indicates high proteoglycan concentration, reinforcing resistance to compressive loads (Utreja *et al*., 2016; Chen *et al*., 2020).

Guinea pigs showed an organization similar to rabbits but with smaller overall thickness and significantly higher cellular density, especially in the TrZ (isogenous groups of 2 - 4 cells, intense purple metachromasia). The RZ had the best columnar organization among species, with gradual transition to a continuous, symmetrical CC, features that may offer an optimal combination of stiffness and elasticity, relevant for studies of chondrogenesis and cartilage repair (Roberts & Goodacre, 2020).

Rats displayed less distinct zonation: a thin TZ (1 - 2 fibroblast layers), a TrZ with small isogenous groups and faint metachromasia, virtually absent columnar organization, and a diffuse, poorly delimited CC. This intermediate pattern suggests lower ability to sustain high, prolonged loads, while retaining some adaptability under experimental conditions.

Mice exhibited the simplest, most homogeneous MC, with the thinnest cartilage and limited zonal organization. The TZ was absent or poorly developed in most samples; the TrZ, despite intense metachromasia, was thin; and the RZ showed short, weakly defined columns, features consistent with adaptation to lower-magnitude, shorter-

duration loads and the lower masticatory demand of this species (Liang *et al*., 2016).

In this context, the intensity and distribution of metachromasia across condylar zones are direct indicators of proteoglycan content and, therefore, of mechanical support capacity and maturational state. The primary role of mandibular condylar cartilage is to sustain and distribute functional loads during mastication, speech, and parafunctional movements, ensuring smooth displacement and minimizing tissue wear (Chen *et al*., 2020). This capacity depends largely on extracellular matrix integrity and, in particular, proteoglycan content and distribution. The heterogeneous distribution observed here suggests species-specific biomechanical adaptations. Rabbits and guinea pigs showed the highest proteoglycan concentrations—evidenced by intense, homogeneous metachromasia, indicating greater damping and efficient load distribution. Given that reduced proteoglycan synthesis (with aging or osteoarthritis) undermines structural integrity and compressive resistance (Chen *et al*., 2020), these differences are highly relevant.

Moreover, the TZ of condylar cartilage exhibits distinctive features likely related to its embryologic origin. Immunohistochemical studies have demonstrated that the articular surface of the MC corresponds to periosteum rather than true cartilage (Shibata *et al*., 2014). This fibrous periosteum in the synovial surfaces of the condyle contains a subadjacent proliferative zone that transforms into a supporting fibrocartilaginous layer, which can subsequently mineralize to form endochondral bone (Shibata *et al*., 2014; Stocum & Roberts, 2018; Roberts & Goodacre, 2020). This arrangement reflects its particular development and helps explain the adaptive and regenerative capacity of the condyle under species-specific functional and mechanical demands.

Functional and Biomechanical Implications

Interspecies differences in morphology and histological organization of the TMJ directly influence load distribution and absorption during mandibular function. In rabbits and guinea pigs, the combination of high collagen density, abundant proteoglycans, and well-defined zonation allows more efficient stress distribution, reducing the risk of structural damage under high demand.

In contrast, in rats and mice, lower zonal differentiation and thinner condylar cartilage suggest reduced capacity to withstand prolonged or high-magnitude loads, potentially explaining greater susceptibility to degeneration in overload models, consistent with reports that proteoglycan loss and collagen disorganization are early events in osteoarthritis progression (Liang, 2016; Chen *et al*., 2020). Fiber orientation—clearly parallel to the articular surface in rabbits but looser in mice, also influences abrasion and friction resistance, critical for condylar durability. These differences should be considered when selecting an animal model for studies of biomaterials, regenerative therapies, or biomechanical interventions. Likewise, the more evident regional specialization in larger species (rabbit, guinea pig) versus greater uniformity in smaller species (mouse) should guide protocols requiring region-specific analyses.

Relevance for Animal Model Selection

Our results provide a robust comparative framework for selecting the most appropriate animal model according to the research question in TMJ studies.

Rabbit: Thick condylar cartilage, high collagen density, and clear zonation make it suitable for advanced degenerative pathology (e.g., osteoarthritis), biomaterial testing, and regenerative techniques under high biomechanical demand; also appropriate for adaptive remodeling studies.

Guinea pig: High cellular density and the most defined columnar organization make it promising for studies on chondrogenesis, repair mechanisms, and therapies promoting chondrocyte proliferation/differentiation; its relatively symmetrical anteroposterior organization favors regional comparisons.

Rat: Intermediate condylar architecture and notable asymmetry make it useful for malocclusion studies, adaptation to abnormal loads, and the effects of occlusal alterations; availability and cost favor exploratory or long-term designs.

Mouse: Despite simple structure, it is invaluable due to transgenic/knockout lines enabling investigation of genetic and molecular mechanisms of homeostasis and degeneration; histological uniformity may facilitate interpretation in basic mechanistic studies, though biomechanical limitations must be considered.

Overall, there is no universal animal model for TMJ research; selection should balance histological features, functional demands, and specific study objectives.

Methodological Considerations and Limitations

A strength of this study is the use of standardized histological protocols enabling direct interspecies comparisons. However, the exclusive inclusion of juvenile

animals' limits extrapolation to later life stages, in which aging and degeneration significantly modify TMJ composition and architecture (Bae, 2003; Liang *et al*., 2016; Yang *et al*., 2023). Structural and molecular changes, reduced proteoglycan secretion, lower cellular density, matrix disorganization, increased proteolytic activity, and altered signaling, are hallmarks of age-related mandibular cartilage degeneration (Chen *et al*., 2020).

Another limitation is the lack of direct functional correlation between histology and quantitative biomechanical parameters (e.g., elastic modulus, compressive strength) that could objectively confirm inferences from microscopy. Nor did we assess molecular markers linking tissue structure with metabolic activity in condylar cartilage and the AD.

Perspectives and Future Directions

The histological differences identified here open several avenues to understand structure–function relationships in the TMJ more precisely. A priority is to establish quantitative correlations between histological features and biomechanical performance of condylar cartilage and the AD, incorporating techniques such as nanoindentation or load-distribution analysis. This would validate whether zonation patterns, collagen organization, or proteoglycan content translate into measurable functional differences under physiological or pathological loading.

A further priority is addressing the lack of consensus on a unified nomenclature for TMJ articular cartilage zones. Although the international histological terminology for humans (FICAT, 2008) and the veterinary counterpart (ICVHN, 2017) share terms for cartilage zones, the scientific literature remains inconsistent. Some authors describe four zones, fibrous tangential, polymorphic, chondrocyte, and hypertrophic chondrocyte (Shibukawa *et al*., 2007), whereas others, particularly in therapeutic studies, focus on cellular features without stratification (Köhnke *et al.*, 2021; Wang *et al.*, 2021). Earlier descriptions even used historical terms such as "perichondrium" for the TZ (Luder *et al*., 1988). More recent work employs a four-zone scheme—superficial, middle, deep, and calcified, that facilitates correlation between histology and biomechanics (Iturriaga *et al*., 2021; Wen *et al*., 2023). We consider it necessary to review and update official terms for both humans and animals, as current nomenclature does not optimally reflect contemporary histology nor facilitate cross-study comparisons. Updating terminology in line with FIPAT (2019) would integrate histological and functional criteria, improving scientific communication and comparative interpretation across disciplines and species.

Zonal molecular profiling is also a promising avenue: differential expression of collagens (types I, II, III, X), aggrecans, metalloproteinases, and other synthesis/degradation markers across zones and species could yield decisive insight into mechanisms that maintain or compromise joint integrity and could link structural findings with specific molecular pathways, opening possibilities for targeted therapies.

Longitudinal designs spanning life stages would clarify how baseline differences influence aging patterns and degeneration, informing the suitability of each model in age-related pathology (e.g., osteoarthritis). Induced-pathology models (mechanical overload, occlusal imbalance, experimental osteoarthritis) could test whether baseline structural features condition degenerative response and repair capacity, explaining interspecies variability in therapeutic outcomes.

Advanced imaging, such as 3D confocal stereology and micro-CT, would enable volumetric assessment of fibrocartilage and subchondral bone microarchitecture with resolution unattainable by 2D methods. Integrating structural, functional, and molecular datasets will foster a multidimensional understanding of the TMJ. Finally, extending this comparative analysis to other common biomedical species (e.g., dog, pig) could broaden available options and improve model selection for specific pathologies or surgical procedures.

CONCLUSIONS

This study provides a comparative histological characterization of the MF, AD, and MC in rabbit, guinea pig, rat, and mouse, revealing relevant morphological and staining differences that reflect species-specific functional and biomechanical adaptations.

We identified a structural-complexity gradient from rabbit (greater cartilage thickness, fibrillar complexity, and defined zonation) to mouse (simpler, more homogeneous morphology). Guinea pigs stood out for high cellular density and well-defined columnar organization, whereas rats showed an intermediate structure with marked condylar asymmetry.

The distribution and intensity of metachromasia, indirect indicators of proteoglycan content, varied among species in ways that correlate with damping capacity and resistance to mechanical loads. Collagen organization and orientation, observed with Picrosirius red, also revealed species-specific patterns associated with functional demands.

These findings provide a solid morphological basis for informed selection of animal models in TMJ research. Model choice should consider not only anatomy but also correspondence between histological features and the pathology or intervention under study.

Finally, this characterization lays the groundwork for future investigations integrating molecular and biomechanical analyses, as well as age-dependent and pathological changes, to optimize translation of experimental results to clinical practice.

NAVARRETE, J.; MENDOZA, F.; ITURRIAGA, V.; WEN, S & VÁSQUEZ, B. Comparación morfocuantitativa de la articulación temporomandibular en especies de laboratorio: conejo, cuye, rata y ratón. *Int. J. Morphol., 43(4)*:1388-1401, 2025.

RESUMEN: La articulación temporomandibular (ATM) es una estructura frecuentemente comprometida por trastornos temporomandibulares (TTM). La elección del modelo animal debe basarse en características morfológicas comparables con la ATM humana, aunque existen pocos estudios comparativos detallados entre especies utilizadas en laboratorio. El objetivo fue comparar histológica y morfométricamente la ATM de conejo, cuye, rata y ratón, para identificar diferencias estructurales relevantes que orienten la elección de modelos animales en investigaciones sobre TTM. Se utilizaron ATMs de cuatro especies (n = 4 ATMs por grupo), mantenidas bajo condiciones controladas. Tras la eutanasia, las muestras fueron fijadas, descalcificadas (EDTA 10 %) y procesadas histológicamente. Se obtuvieron cortes parasagitales (5 µm), teñidos con azul de toluidina y Picrosirius red. El análisis histológico se enfocó en la fosa mandibular (FM), disco articular (DA) y cóndilo mandibular (CM). Se aplicó un protocolo morfométrico estandarizado para medir el grosor total en las regiones anterior (RA), media (RM) y posterior (RP) y en las zonas tangencial (ZT), transicional (ZTr), radial (ZR) y cartílago calcificado (CC) del cartílago condilar en las tres regiones anatómicas. Las especies mostraron diferencias en zonificación del cartílago, densidad celular y organización estructural. Conejo y cuye presentaron una organización zonal bien definida y mayor tinción catiónica de matriz. Rata y ratón exhibieron menor diferenciación zonal. Con Picrosirius red, conejo y cuye mostraron birrefringencia intensa en DA; enel ratón fue débil y dispersa. Morfométricamente, el conejo mostró en general los mayores espesores y el ratón los menores, aunque cada especie presentó un patrón regional único. El conejo destacó por registrar los máximos valores en la ZR y CC en todas las regiones. Las diferencias histoarquitectónicas y morfométricas reflejan adaptaciones biomecánicas específicas. Conejos y cuyes serían más apropiados para estudios de alta carga y fibrocartílago complejo; la rata, por su estructura intermedia y asimetría condilar, sería útil en investigaciones de adaptación mecánica y maloclusión; mientras que el ratón es adecuado para estudios genéticos y moleculares por su homogeneidad estructural y disponibilidad de modelos transgénicos.

PALABLAS CLAVE: Articulación temporomandibular; histología; Morfometría; Modelos animales.

REFERENCES

Bae, J. W.; Takahashi, I.; Sasano, Y.; Onodera, K.; Mitani, H.; Kagayama, M. & Mitani, H. Age-related changes in gene expression patterns of matrix metalloproteinases and their collagenous substrates in mandibular condylar cartilage in rats. *J. Anat., 203(2)*:235-41, 2023.

Bechtold, T. E.; Saunders, C.; Decker, R. S.; Um, H. B.; Cottingham, N.; Salhab, I.; Kurio, N.; Billings, P. C.; Pacifici, M.; Nah, H. D. & Koyama, E. Osteophyte formation and matrix mineralization in a TMJ osteoarthritis mouse model are associated with ectopic hedgehog signaling. *Matrix Biol., 52-54*:339-54, 2016.

Berkovitz, B. K. Crimping of collagen in the intra-articular disc of the temporomandibular joint: a comparative study. *J. Oral Rehabil., 27(7)*:608-13, 2000.

Chen, P. J.; Dutra, E. H.; Mehta, S.; O'Brien, M. H. & Yadav, S. Age-related changes in the cartilage of the temporomandibular joint. *Geroscience, 42(3)*:995-1004, 2020.

Cougo, M. C. R.; Quevedo, A. S. de & Ponzoni, D. Modelos animais utilizados para o estudo da articulação temporomandibular?: revisão de literatura. *Res. Soc. Dev., 10(12)*:e420101220586, 2021.

Dellavia, C.; Rodella, L. F.; Pellecchia, R. & Barzani, G. *Detailed Anatomy of the Temporomandibular Joint*. In Connelly, S. T.; Tartaglia, G. M. & Silva, R. G. (Eds.), Contemporary Management of Temporomandibular Disorders: Fundamentals and Pathway to Diagnosis. Cham, Springer International Publishing, 2019. pp. 51-70.

Federative International Comittee on Anatomical Terminology (FICAT). *Terminologia Histologica, International Terms for Human Cytology and Histology*. Philadelphia, Wolters Kluwer/ Lippincott Williams & Wilkins, 2008.

Federative International Programme for Anatomical Terminology (FIPAT). *Terminologia Anatomica*. 2nd ed. FIPAT.library.dal.ca. Federative International Programme for Anatomical Terminology, 2019.

Herring, S. W. TMJ anatomy and animal models. *J. Musculoskelet Neuronal Interact., 3(4)*:391-407, 2003.

Herring, S. W.; Decker, J. D.; Liu, Z. J. & Ma, T. Temporomandibular joint in miniature pigs: Anatomy, cell replication, and relation to loading. *Anat Rec., 266(3)*:152-66, 2002.

International Committee on Veterinary Histological Nomenclature. (ICVHN). *Nomina histologica veterinaria* (1st ed.). World Association of Veterinary Anatomists. 2017. Available in: http://www.wava-amav.org/

Institute for Laboratory Animal Research. *Guide for the Care and Use of Laboratory Animals*. National Academies Press, Washington, DC, USA, 2011.

Iturriaga, V.; Vásquez, B.; Bornhardt, T. & del Sol, M. Effects of low and high molecular weight hyaluronic acid on the osteoarthritic temporomandibular joint in rabbit. *Clin. Oral Investig., 25(7)*:4507-18, 2021.

Jung, J. K.; Sohn, W. J.; Lee, Y.; Bae, Y. C.; Choi, J. K. & Kim, J. Y. Morphological and cellular examinations of experimentally induced malocclusion in mice mandibular condyle. *Cell Tissue Res., 355(2)*:355-63, 2014.

Köhnke, R.; Ahlers, M. O.; Birkelbach, M. A.; Ewald, F.; Krueger, M.; Fiedler, I.; Busse, B.; Heiland, M.; Vollkommer, T.; Gosau, M.; Smeets, R. & Rutkowski, R. Temporomandibular joint osteoarthritis: Regenerative treatment by a stem cell containing advanced therapy medicinal product (ATMP)—An *in vivo* animal trial. *Int. J. Mol. Sci., 22*:443, 2021.

Liang, W.; Li, X.; Gao, B.; Gan, H.; Lin, X.; Liao, L. & Li, C. Observing the development of the temporomandibular joint in embryonic and post-natal mice using various staining methods. *Exp. Ther. Med., 11(2)*:481-9, 2016.

Luder, H. U. Age changes in the articular tissue of human mandibular condyles from adolescence to old age: a semiquantitative light microscopic study. *Anat. Rec., 251(4)*:439-47, 1998.

Matamala, V. F.; Fuentes, F. R. & Ceballos, C. M. Morfología y morfometría del disco de la articulación témporomandibular en fetos y adultos humanos. *Int. J. Morphol., 24(2)*:245-50, 2006.

Nanci, A. *Ten Cate's oral histology: Development, structure, and function* (9. éd.). St. Louis, MO, Elsevier, 2018.

Okeson, J. P. *Management of temporomandibular disorders and occlusion.* 7th ed. St.Louis, MO, Elsevier/Mosby, 2013.

Palla, S. *Anatomy and pathophysiology of the temporomandibular joint.* In: Klineberg, I. & Eckert, S. E. (eds.) Functional Occlusion in Restorative Dentistry and Prosthodontics. Edinburgh, Elsevier/Mosby, 2016. pp. 67-85.

Porto, G.; Vasconcelos, B. C.; Andrade, E. S. & Silva-Junior, V. A. Comparison between human and rat TMJ: anatomic and histopathologic features. *Acta Cir. Bras., 25(3)*:290-3, 2010.

Roberts, W. E. & Goodacre, C. J. The Temporomandibular Joint: A Critical Review of Life-Support Functions, Development, Articular Surfaces, Biomechanics and Degeneration. *J. Prosthodont., 29(9)*:772-9, 2020.

Russell, W. M. S. & Burch, R. L. *The Principles of Humane Experimental Technique;* Universities Federation for Animal Welfare: Wheathampstead, UK, 1959; reprinted in 1992.

Shibukawa, Y.; Young, B.; Wu, C.; Yamada, S.; Long, F.; Pacifici, M. & Koyama, E. Temporomandibular joint formation and condyle growth require Indian hedgehogsignaling. *Dev. Dyn., 236(2)*:426-34, 2007.

Shibata, S.; Sakamoto, Y.; Yokohama-Tamaki, T.; Murakami, G. & Cho, B. H. Distribution of Matrix Proteins in Perichondrium and Periosteum During the Incorporation of Meckel's Cartilage into Ossifying Mandible in Midterm Human Fetuses: An Immunohistochemical Study. *Anat. Rec. (Hoboken), 297(7)*:1208-17, 2014.

Stocum, D. L. & Roberts, W. E. Part I: Development and Physiology of the Temporomandibular Joint. Curr .*Osteoporos. Rep., 16(4)*:360-8, 2018.

Suzuki, A. & Iwata, J. Mouse genetic models for temporomandibular joint development and disorders. *Oral Dis., 22(1)*:33-8, 2016.

Tomas, X.; Pomes, J.; Berenguer, J.; Mercader, J. M.; Pons, F. & Donoso, L. Temporomandibular joint soft-tissue pathology, II: Nondisc abnormalities. *Semin. Ultrasound CT MR., 28(3)*:205-12, 2007.

Tomasello, G.; Sorce, A.; Mazzola, M.; Barone, R.; Lo Piccolo, C.; Farina, F.; Zummo, G. & Carini, F. Comparative analysis of the structure of temporomandibular joint in human and rabbit. *Acta Biomed., 87(3)*:282-5, 2016.

Ukita, M.; Matsushita, K.; Tamura, M. & Yamaguchi, T. Histone H3K9 methylation is involved in temporomandibular joint osteoarthritis. *Int. J. Mol. Med., 45(2)*:607-14, 2020.

Utreja, A.; Dyment, N. A.; Yadav, S.; Villa, M. M.; Li, Y.; Jiang, X.; Nanda, R. & Rowe, D. W. Cell and matrix response of temporomandibular cartilage to mechanical loading. *Osteoarthritis Cartilage., 24(2)*:335-44, 2016.

Wang, Y.; Zhao, M.; Li, W.; Yang, Y.; Zhang, Z.; Ma, R. & Wu, M. BMSC-Derived small extracellular vesicles induce cartilage reconstruction of temporomandibular joint osteoarthritis via autotaxin-YAP signaling axis. *Front. Cell Dev. Biol., 9*:656153, 2021.

Wen, S.; Iturriaga, V.; Vásquez, B. & del Sol, M. Comparison of four treatment protocols with intra-articular medium molecular weight hyaluronic acid in induced temporomandibular osteoarthritis: an experimental study. *Int. J. Mol. Sci., 24(18)*:14130, 2023.

Wurgaft, R. & Montenegro, M. *Desarrollo y estructura de la articulación temporomandibular.* Santiago, Servimpres Ltda., 2003.

Yang, M. C.; Nakamura, M.; Kageyama, Y.; Igari, Y. & Sasano, Y. Age-related gene and protein expression in mouse mandibular condyle analyzed by cap analysis of gene expression and immunohistochemistry. *Gerontology, 69(11)*:1295-1306, 2023.

Zhao, Y.; An, Y.; Zhou, L.; Wu, F.; Wu, G.; Wang, J. & Chen, L. Animal models of temporomandibular joint osteoarthritis: classification and selection. *Front. Physiol., 13*:859517, 2022.

Corresponding author:
Dra. Bélgica Vásquez
Center of Excellence in Morphological and Surgical Studies
Universidad de La Frontera
Temuco
CHILE

E-mail: belgica.vasquez@ufrontera.cl

ORCID: https://orcid.org/0000-0002-4106-3548